LAWRENCE
LIVERMORE
NATIONAL
LABORATORY

UCRL-JRNL-229513

Formation, Stability, and Mobility of One-Dimensional Lipid Bilayer on High Curvature Substrates

Jay Huang, Julio Martinez, Alexander Artyukhin, Donald Sirbuly, Yinmin Wang, Jian Wen Ju, Pieter Stroeve, Aleksandr Noy

March 28, 2007

Nano Letters

Formation, Stability, and Mobility of One-Dimensional Lipid Bilayer on High Curvature Substrates

Shih-Chieh J. Huang[1,2], Julio A. Martinez[1,3], Alexander B. Artyukhin[1,3], Donald J. Sirbuly[1], Jiann-Wen Ju[2], Pieter Stroeve[3], Aleksandr Noy[1*]

[1] Chemistry, Materials, and Life Sciences Directorate, Lawrence Livermore National Laboratory, Livermore, CA 94550, [2] Department of Civil and Environmental Engineering, University of California Los Angeles, Los Angeles, CA 90095, [3] Department of Chemical Engineering and Materials Science, University of California Davis, Davis, CA 95616

[*] Corresponding author, noy1@llnl.gov

ABSTRACT

Curved lipid membranes are ubiquitous in living systems and play an important role in many biological processes. To understand how curvature and lipid composition affect membrane formation and fluidity we have assembled and studied mixed 1,2-Dioleoyl-sn-Glycero-3-Phosphocholine (DOPC) and 1,2-Dioleoyl-sn-Glycero-3-Phosphoethanolamine (DOPE) supported lipid bilayers on amorphous silicon nanowires with controlled diameters ranging from 20 nm to 200 nm. Addition of cone-shaped DOPE molecules to cylindrical DOPC molecules promotes vesicle fusion and bilayer formation on smaller diameter nanowires. Our experiments demonstrate that nanowire-supported bilayers are mobile, exhibit fast recovery after photobleaching, and have low concentration of defects. Lipid diffusion coefficients in these high-curvature tubular membranes are comparable to the values reported for flat supported bilayers and increase with decreasing nanowire diameter.

Lipid membranes of non-planar shapes are abundant in nature. Numerous reports document their existence in cellular organelles and transient formation in various biological processes.[1-6] Nonetheless, researchers became interested in the

role of the membrane curvature in biology only recently,[7, 8] and quickly realized that they need to understand how curvature affects structure and physical properties of the membrane.[9, 10] Recent experiments demonstrated curvature-directed segregation of lipid mixtures in membranes of variable curvature.[11-13] Fluidity is another critical parameter of biological membranes, since mobility of lipids and membrane proteins represents one of the key factors in regulating ligand-receptor interactions, cooperative binding, and aggregation.[14, 15] Earlier experiments on silica bead-supported lipid bilayers[16, 17] indicated that substrate curvature does not significantly influence diffusion of lipid molecules for the substrate diameters larger than 0.5 μm. However, biological membranes frequently form tubular shapes[1, 3, 18-20] with the radii between 10 and 100 nm; yet there are no systematic literature data on lipid mobility for membranes with the radius of curvature smaller than 100 nm. We intuitively expect that differences in packing densities between highly curved and planar membranes would affect membrane fluidity; therefore it is necessary to study the lipid membrane structure and mobility in the high-curvature regime.

Here we report formation and mobility of mixed zwitterionic (DOPC and DOPE) lipid bilayers of different compositions supported on cylindrical hydrophilic nanowire substrates with diameters ranging from 20 to 200 nm. These experiments demonstrate how the size of the headgroup and the overall shape of lipid molecules changes bilayer stability and its ability to fuse on non-planar substrates. Finally, we use Fluorescence Recovery After Photobleaching (FRAP) technique to study the lipid mobility at different substrate curvatures and

show that for all bilayer compositions the lipid mobility increases with the decreasing radius of curvature.

Substrate design and fabrication. To characterize membrane properties as a function of curvature we need to prepare bilayers with measurable, reproducible, and well controlled curvature. Non-planar free standing bilayers, i.e. lipid vesicles, typically do not meet these criteria. Although lipid vesicles are easy to prepare, all existing methods give wide, non-uniform distribution of vesicle sizes (and thus curvatures). Our approach utilizes assembly of lipid bilayers on solid substrates of variable curvature. Supported bilayer membranes retain many similarities to natural membranes, and most importantly, lateral fluidity.[21] Our substrates consist of cylindrical amorphous silicon nanowires (with native silicon oxide surface) grown over small diameter carbon nanotubes and suspended over a microfabricated trench on a silicon wafer (Figure 1). The outer diameter of these core-shell nanostructures then defines the membrane curvature. Suspended nanowire "bridge" geometry allows for the formation of a cylindrical lipid membrane of the well defined shape and curvature along the entire nanowire length. We chose to use these support surfaces also because of the well-known ability of the silicon oxide to promote fusion of lipid vesicles to form fluid supported bilayers.[22]

Our nanowire fabrication starts with CVD growth of single-walled carbon nanotubes suspended across microfabricated channels in Si/SiO_2 (Figure 1a, step 1. See Supporting Information for details). These suspended nanotubes serve as templates for growing a layer of amorphous silicon (Figure 1a, step 2), which produces 5 μm long cylindrical silicon wires of 20 – 200 nm in diameter (Figure

1b,c). This fabrication process is very reproducible. For our studies we have fabricated nanowires with ultra-narrow diameter distributions and smooth walls (the average width of the diameter distributions was 1.7±0.9% and the maximum peak-to-valley surface roughness of the nanowire surface was less that 2 nm). The uniformity of the nanowire substrates produced by our synthesis procedure provides a key advantage for studying curvature effects in supported lipid bilayers. In comparison, catalytic CVD synthesis produces single-crystalline silicon nanowires[23] with atomically smooth surfaces; however the nanowire diameter distribution in CVD samples is usually quite broad,[24] which would complicate correlation of membrane properties with the substrate curvature.

Vesicle fusion on curved substrates. To explore relationship between the shape of lipid molecules and the membrane curvature[25] we have studied fusion of mixed DOPE-DOPC vesicles on nanowires of various diameters using confocal fluorescence microscopy (Figure 2, 4a). To visualize formation of supported lipid bilayers we added 2 % of a fluorescent probe 1-Oleoyl-2-[6-[(7-nitro-2-1,3-benzoxadiazol-4-yl)amino]hexanoyl]-*sn*-Glycero-3-Phosphoethanolamine (NBD-PE) to all lipid compositions. When we exposed silicon nanowires to lipid vesicles (Figure 1a, step 3) the vesicles readily fused onto these substrates producing linear bright fluorescent features in the confocal microscopy images (Figure 2b-d). Remarkably, we observed that for all lipid compositions that we studied the vesicles did not fuse onto all the substrates; rather, vesicles of each lipid composition only fused on the nanowires in a limited range of diameters (Table 1). In general, the increase in DOPE fraction in the lipid mixture shifted the nanowire diameter range where vesicles successfully fuse to smaller values (Table

1). Moreover, the lipid vesicles with higher DOPE content that selectively coated smaller diameter nanowires did not fuse on a planar surface (Figure 2d). This observation is consistent with the ability of conical DOPE to inhibit lipid bilayer formation on flat glass substrates.[25]

We can explain the observed effects if we consider the shapes of the lipid molecules. Due to the difference in chemical structure of the headgroups PC lipids are cylindrical, while PE lipids are truncated cones (Figure 2a). As a result, different mixtures of these lipids have different intrinsic curvatures. Hamai et al. reported that with increasing DOPE concentration in DOPC-DOPE vesicles the mobile fraction of supported lipid bilayers on flat surfaces dropped and fluorescence signal stopped to recover when the fraction of DOPE reached 20 %.[25] The authors reported that vesicles of this composition adsorbed on the flat substrates without fusion and bilayer formation. Our results clearly demonstrate that it is possible to form *mobile* supported bilayers on curved surfaces of cylindrical nanowires even at DOPE fraction larger than 20 % (Table 1).

Thermodynamics of bilayer formation. To rationalize our results we need to consider thermodynamics of the bilayer formation on a curved surface. The free energy of the bilayer formation ΔG includes two components: (1) the bending energy ΔE_{bend} required to deform the membrane to the nanowire shape and the adhesion energy of the lipid headgroups to the silicon oxide surface, ΔE_{adh}:[26, 27]

$$\Delta G = \Delta E_{bend} - \Delta E_{adh} . \quad (1)$$

The bending energy per unit area of the lipid membrane is equal to[25]

$$\Delta E_{bend} = \frac{k}{2} \cdot \left(\frac{1}{R} - J_0 \right)^2, \qquad (2)$$

where k and J_0 are the stiffness coefficient and the intrinsic curvature of the lipid monolayer, respectively.[8] Lipid curvature is positive when headgroups are pointing outward away from the center of the curvature, and negative when headgroups are pointing inwards toward the center. Thus, inner and outer leaflets of a non-planar bilayer have opposite curvatures and make different contributions to the bending energy term. The total bending energy of a cylindrical bilayer then becomes (see Figure 3a for an additional explanation of the geometrical parameters):

$$\Delta E_{bend} = L \cdot \left(2\pi \cdot R \cdot \frac{k}{2} \cdot \left(\frac{1}{R} + J_0 \right)^2 + 2\pi \cdot (R+h) \cdot \frac{k}{2} \cdot \left(\frac{1}{R+h} - J_0 \right)^2 \right) \qquad (3)$$

where L and R are the length and the radius of the nanowire template; h *is* the thickness of the lipid monolayer. To calculate the bending energy term we used values of h=2 nm and k=3.9·10^{-20} J,[28-32] for both lipids in our calculations. For each DOPC-DOPE mixture we calculated the effective intrinsic curvature of both inner and outer leaflets using a linear combination[25] of intrinsic curvatures for pure DOPC and DOPE monolayers (-0.05 and -0.33 nm^{-1}, respectively).[8, 33] Note that the lipid distribution between two monolayers is not necessarily symmetrical: due to their conical shape DOPE molecules should preferentially reside in the inner (closer to the nanowire) leaflet of the bilayer.[34] Such redistribution of the lipid molecules between the two leaflets according to their molecular shape lowers the bending energy of the system. We calculated the equilibrium DOPE distribution between the monolayers by minimizing the total

bending energy for each nanowire diameter. As a result, DOPE concentration is higher than the nominal in the inner leaflet and lower in the outer one. In fact, our estimates show that for nanowires smaller than 30 and 55 nm in diameter for DOPC:DOPE of 70:30 and 80:20, respectively all DOPE will concentrate in the inner monolayer.

The adhesion energy for a lipid bilayer fused onto a cylinder of radius R and length L is equal to

$$\Delta E_{adh} = 2\pi \cdot L \cdot R \cdot C_{adh} \quad (4)$$

where C_{adh} is the adhesion coefficient between the lipid and a silicon oxide surface.[26, 35] Using C_{adh} = $1.0 \cdot 10^{-4}$ J/m^2,[26, 36, 37] for both DOPC and DOPE we calculated the free energy of the lipid bilayer formation as a function of the substrate radius for each lipid mixture (Figure 3b-d, lines). Remarkably, the calculated bilayer formation energies readily explain the trends observed in the fusion experiments. For all bilayer compositions the nanowire sizes that produced fused bilayers in the experiments cluster around the minimum on the calculated free energy curves while the nanowire sizes where the bilayers do not form are further away from the minimum. Note also that in the case of pure DOPC (Figure 3b), the energy curve does not have a minimum indicating that the flat bilayer represents the lowest energy configuration for that membrane.

Lipid mobility. Lipid membranes adsorbed on curved substrates are highly mobile. We have measured the diffusion coefficients of lipid molecules in these membranes using FRAP technique, where we used a high-power focused laser beam to bleach a small spot on the bilayer-coated nanowire and then monitored lipid diffusion back into the bleached region.[38, 39] To achieve the time resolution

necessary for capturing the recovery process, our setup incorporated an electro-optical modulator (Figure 4a) that could switch the power of the laser beam in less than 2 μs.

Most of our 1-D bilayer membranes exhibited mobile fractions of nearly 100% (Figure 4b), even for membranes that contained 20-30 % of DOPE. Note the striking contrast of these results with the previous studies that show that DOPE concentrations higher than 20 % produce immobile lipid on flat glass surfaces.[25] Moreover, our supported bilayers are highly robust: we obtained fluorescence recovery of 90-95 % on the coated nanowires even after 5 bleach-recovery cycles on the same spot (data not shown).

To extract diffusion coefficients from the recovery data we used a one-dimensional diffusion model.[39] Our results (Table 1) show that our membranes are remarkably mobile: the diffusion coefficients of nanowire supported membranes fall in the range of values reported for DOPC vesicles ($5 \cdot 10^{-8}$ cm^2/s)[40] and flat supported DOPC bilayers($2\text{-}3 \cdot 10^{-8}$ cm^2/s).[25, 41] This high mobility is in sharp contrast to the reported mobilities of one-dimensional lipid bilayers on carbon nanotube templates coated with polyelectrolytes.[39] These substrates were of comparable size to the smallest nanowires used in the present work, yet they exhibited diffusion coefficients that were three orders of magnitude slower. This comparison indicates that the nature of the substrate surface represents another key factor that determines the bilayer mobility on highly curved substrates.

Our experiments also showed that for each DOPC-DOPE mixture the mobility gradually increases by a factor of 1.5-4 with decreasing nanowire diameter in the range 20-200 nm. Similarly, Hof et al. found that relaxation time

of a fluorescent probe was approximately twice as short in small vesicles (diameter 22 nm) compared to large ones (diameter 250 nm).[42]

Our data support the explanation proposed by Hof and colleges.[42] As the membrane curvature increases, the separation between lipid headgroups in the outer leaflet becomes larger. The reduction of the headgroup packing density in the outer leaflet[43] makes it more disordered. Wider open spaces between headgroups in the lipid bilayers supported on small diameter nanowires facilitate lateral diffusion and result in higher diffusion coefficients. We also note that Hof et al. used the probe that tended to concentrate in the outer leaflet. Our experiments use the probe (NBD-PE) that tends to reside in the inner monolayer. Thus quantitative comparison between our results and data obtained by Hof and colleges is not entirely straightforward.

We have shown that mixed DOPC-DOPE vesicles form supported lipid bilayers on small diameter cylindrical silicon nanowires. The substrate size range where fusion occurs depends on the DOPC:DOPE lipid ratio and reflects the interplay between bilayer adhesion to the substrate surface and the energy required to bend the membrane to the nanowire curvature. By adjusting fraction of cone-shaped DOPE molecules in the lipid mixture we can control the range of nanowire diameters that favor bilayer formation. We demonstrate that lipid bilayers supported on silicon nanowires are high-quality, continuous, and mobile. They exhibit mobile fractions of 90-100 % and diffusion coefficients close to typical values for DOPC membranes supported on flat silicon oxide surfaces. We also found that the membrane mobility increases several times as the nanowires become thinner.

These results open up a number of opportunities for researchers. 1-D bilayers on high-curvature solid supports provide a reliable and robust platform for studying physical properties of the highly-curved lipid bilayers. These nanostructures also enable studies of the lipid bilayer compositions that do not form regular (flat) supported bilayers. The approach that we present is quite general, and should also work for other types of hydrophilic nanowires, demonstrating that one-dimensional lipid bilayers provide a versatile platform for integration of biological membranes with 1-D nanomaterials.

Acknowledgment. S.C.J.H., J.A.M., and A.B.A. acknowledge SEGR Fellowship from LLNL. A.N. acknowledges funding from LLNL LSTO. This work was performed under the auspices of the U.S. Department of Energy by the University of California, Lawrence Livermore National Laboratory, under Contract No. W-7405-Eng-48.

Table 1. Diffusion coefficients ($D \cdot 10^{-8}$ cm^2/s) of NBD-PE fluorescent probe in mixed DOPC-DOPE bilayers supported on amorphous silicon nanowires of different diameters. "**X**" indicates that no fusion was observed for the nanowires of this size.

DOPC:DOPE	Nanowire diameter, nm				
	23	30	55	70	200
100:0	x	x	8.7 ± 0.3	3.8 ± 0.3	2.4 ± 0.2
80:20	x	x	8.5 ± 0.6	2.2 ± 0.3	x
70:30	10.5 ± 0.2	8.8 ± 0.4	7.8 ± 0.1	x	

References.

1. Cluett, E. B.; Wood, S. A.; Banta, M.; Brown, W. J. *J. Cell Biol.* **1993,** *120*, 15.

2. McNiven, M. A.; Thompson, H. M. *Science* **2006,** *313*, 1591.

3. Sciaky, N.; Presley, J.; Smith, C.; Zaal, K. J. M.; Cole, N.; Moreira, J. E.; Terasaki, M.; Siggia, E.; LippincottSchwartz, J. *J. Cell Biol.* **1997,** *139*, 1137.

4. Conner, S. D.; Schmid, S. L. *Nature* **2003,** *422*, 37.

5. Farsad, K.; Ringstad, N.; Takei, K.; Floyd, S. R.; Rose, K.; De Camilli, P. *J. Cell Biol.* **2001,** *155*, 193.

6. Peter, B. J.; Kent, H. M.; Mills, I. G.; Vallis, Y.; Butler, P. J. G.; Evans, P. R.; McMahon, H. T. *Science* **2004,** *303*, 495.

7. McMahon, H. T.; Gallop, J. L. *Nature* **2005,** *438*, 590.

8. Zimmerberg, J.; Kozlov, M. M. *Nature Rev. Mol. Cell Biol.* **2006,** *7*, 9.

9. Kucerka, N.; Pencer, J.; Sachs, J. N.; Nagle, J. F.; Katsaras, J. *Langmuir* **2007,** *23*, 1292.

10. Sykora, J.; Jurkiewicz, P.; Epand, R. M.; Kraayenhof, R.; Langner, M.; Hof, M. *Chem. Phys. Lipids* **2005,** *135*, 213.

11. Roux, A.; Cuvelier, D.; Nassoy, P.; Prost, J.; Bassereau, P.; Goud, B. *The EMBO J.* **2005,** *24*, 1537.

12. Parthasarathy, R.; Yu, C.; Groves, J. T. *Langmuir* **2006,** *22*, 5095.

13. Baumgart, T.; Hess, S. T.; Webb, W. W. *Nature* **2003,** *425*, 821.

14. Schindler, M.; Koppel, D. E.; Sheetz, M. P. *Proc. Natl. Acad. Sci. U.S.A.* **1980,** *77*, 1457.

15. Schlessinger, J.; Shechter, Y.; Cuatrecasas, P.; Willingham, M. C.; Pastan, I. *Proc. Natl. Acad. Sci. U.S.A.* **1978,** *75*, 5353.

16. Kochy, T.; Bayerl, T. M. *Phys. Rev. E* **1993,** *47*, 2109.

17. Picard, F.; Paquet, M. J.; Dufourc, E. J.; Auger, M. *Biophys. J.* **1998,** *74*, 857.

18. de Figueiredo, P.; Drecktrah, D.; Katzenellenbogen, J. A.; Strang, M.; Brown, W. J. *Proc. Natl. Acad. Sci. U.S.A.* **1998,** *95*, 8642.

19. Roux, A.; Cappello, G.; Cartaud, J.; Prost, J.; Goud, B.; Bassereau, P. *Proc. Natl. Acad. Sci. U.S.A.* **2002,** *99*, 5394.

20. Takei, K.; Haucke, V.; Slepnev, V.; Farsad, K.; Salazar, M.; Chen, H.; De Camilli, P. *Cell* **1998,** *94*, 131.

21. Sackmann, E. *Science* **1996,** *271*, 43.

22. Cremer, P. S.; Boxer, S. G. *J. Phys. Chem. B* **1999,** *103*, 2554.

23. Morales, A. M.; Lieber, C. M. *Science* **1998,** *279*, 208.

24. Cui, Y.; Lauhon, L. J.; Gudiksen, M. S.; Wang, J.; Lieber, C. M. *Appl. Phys. Lett.* **2001,** *78*, 2214.

25. Hamai, C.; Yang, T.; Kataoka, S.; Cremer, P. S.; Musser, S. M. *Biophys. J.* **2006,** *90*, 1241.

26. Schonherr, H.; Johnson, J. M.; Lenz, P.; Frank, C. W.; Boxer, S. G. *Langmuir* **2004,** *20*, 11600.

27. Ponnuswamy, A.; Nulton, J.; Mahaffy, J. M.; Salamon, P.; Frey, T. G.; Baljon, A. R. C. *Phys. Biol.* **2005,** *2*, 73.

28. Rawicz, W.; Olbrich, K. C.; McIntosh, T.; Needham, D.; Evans, E. *Biophys. J.* **2000,** *79*, 328.

29. Booth, P. J.; Templer, R. H.; Meijberg, W.; Allen, S. J.; Curran, A. R.; Lorch, M. *Critical Rev. Biochem. Mol. Biol.* **2001,** *36*, 501.

30. Evans, E.; Needham, D. *J. Phys. Chem.* **1987,** *91*, 4219.

31. Attard, G. S.; Templer, R. H.; Smith, W. S.; Hunt, A. N.; Jackowski, S. *Proc. Natl. Acad. Sci. U.S.A.* **2000,** *97*, 9032.

32. Chen, Z.; Rand, R. P. *Biophys. J.* **1997,** *73*, 267.

33. Marsh, D. *Biophys. J.* **1996,** *70*, 2248.

34. Marrink, S. J.; Mark, A. E. *J. Amer. Chem. Soc.* **2003,** *125*, 15233.

35. Deserno, M.; Gelbart, W. M. *J. Phys. Chem. B* **2002,** *106*, 5543.

36. Furukawa, K.; Sumitomo, K.; Nakashima, H.; Kashimura, Y.; Torimitsu, K. *Langmuir* **2007,** *23*, 367.

37. Nissen, J.; Gritsch, S.; Wiegand, G.; Radler, J. O. *Eur. Phys. J. B* **1999,** *10*, 335.

38. Axelrod, D.; Koppel, D. E.; Schlessinger, J.; Elson, E.; Webb, W. W. *Biophys. J.* **1976,** *16*, 1055.

39. Artyukhin, A. B.; Shestakov, A.; Harper, J.; Bakajin, O.; Stroeve, P.; Noy, A. *J. Amer. Chem. Soc.* **2005,** *127*, 7538.

40. Tocanne, J. F.; Dupoucezanne, L.; Lopez, A. *Prog. Lipid Res.* **1994,** *33*, 203.

41. Przybylo, M.; Sykora, J.; Humpolickova, J.; Benda, A.; Zan, A.; Hof, M. *Langmuir* **2006,** *22*, 9096.

42. Hof, M.; Hutterer, R.; Perez, N.; Ruf, H.; Schneider, F. W. *Biophys. Chem*. **1994,** *52*, 165.

43. Brouillette, C. G.; Segrest, J. P.; Ng, T. C.; Jones, J. L. *Biochemistry* **1982,** *21*, 4569.

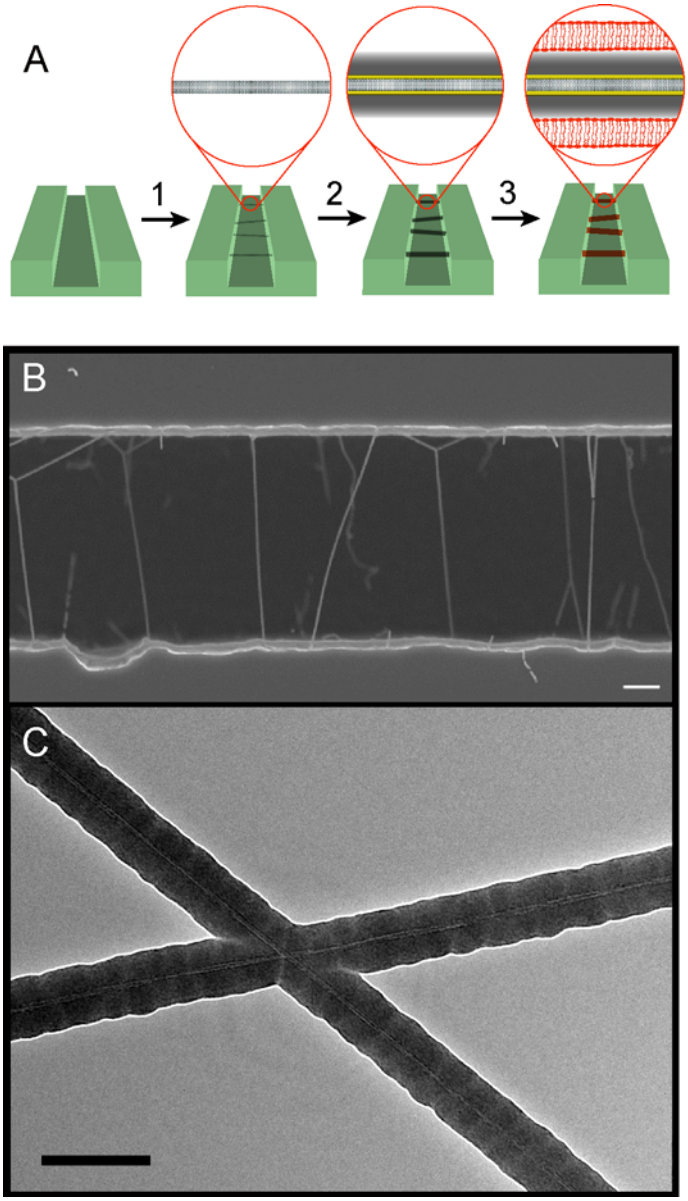

Figure 1. Silicon-coated carbon nanotubes as substrates for studying 1-D lipid membranes. (**A**) Assembly of lipid bilayer membranes on silicon nanowires. Step 1: CVD growth of suspended carbon nanotubes; Step 2: deposition of Ti adhesion layer and amorphous silicon on carbon nanotubes; Step 3: formation of supported bilayer by vesicle fusion. (**B**) SEM image of silicon coated carbon nanotubes suspended over a 5 μm-wide channel. (**C**) TEM image of two silicon coated carbon nanotubes. The nanotubes represented on this image formed a cross-junction before amorphous silicon deposition. Scale bars: 1 μm (B), 100 nm (C).

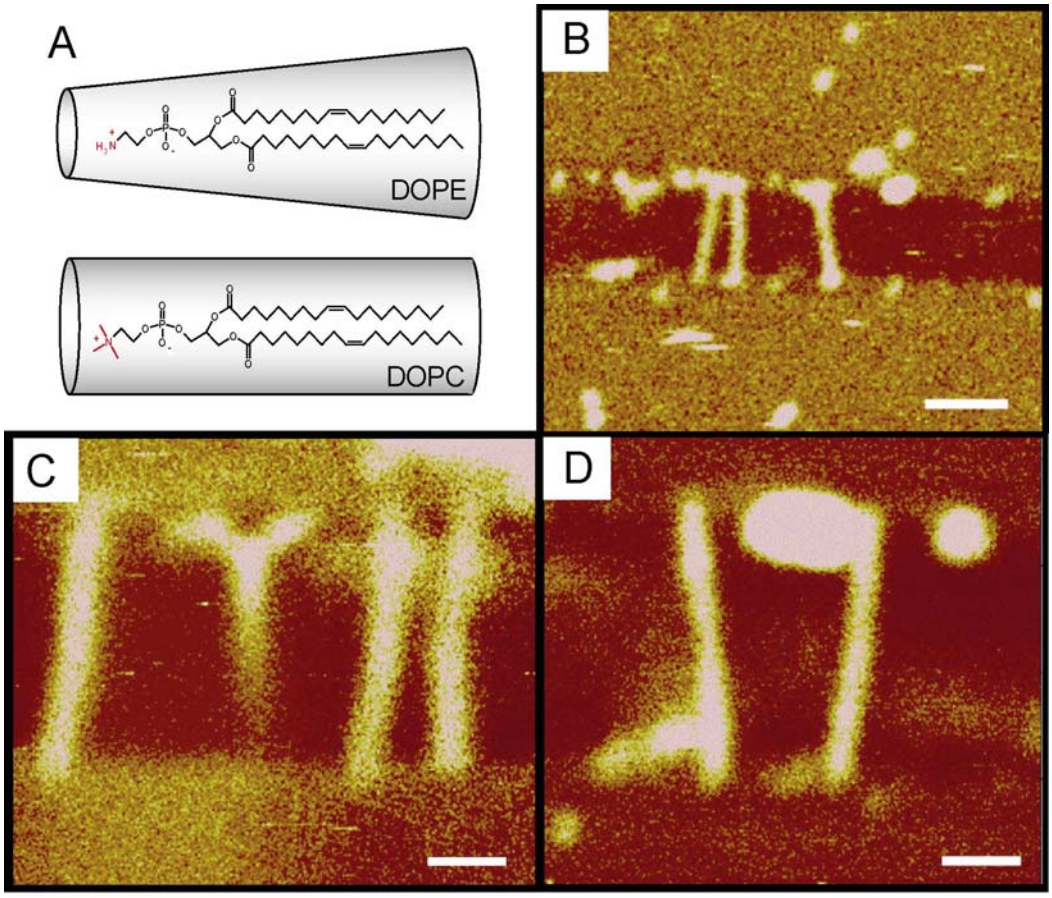

Figure 2. (**A**) Structural formulae and overlaid schematic representation of the geometrical shapes of DOPC and DOPE lipid molecules. (**B**-**D**) Confocal fluorescence microscopy images of lipid bilayers supported on silicon nanowires. DOPC:DOPE ratio was 100:0 (**B**), 80:20 (**C**), and 70:30 (**D**). Nanowire diameters were 70 nm (B, C) and 55 nm (D). Scale bars: 5 μm (B), 2 μm (C, D).

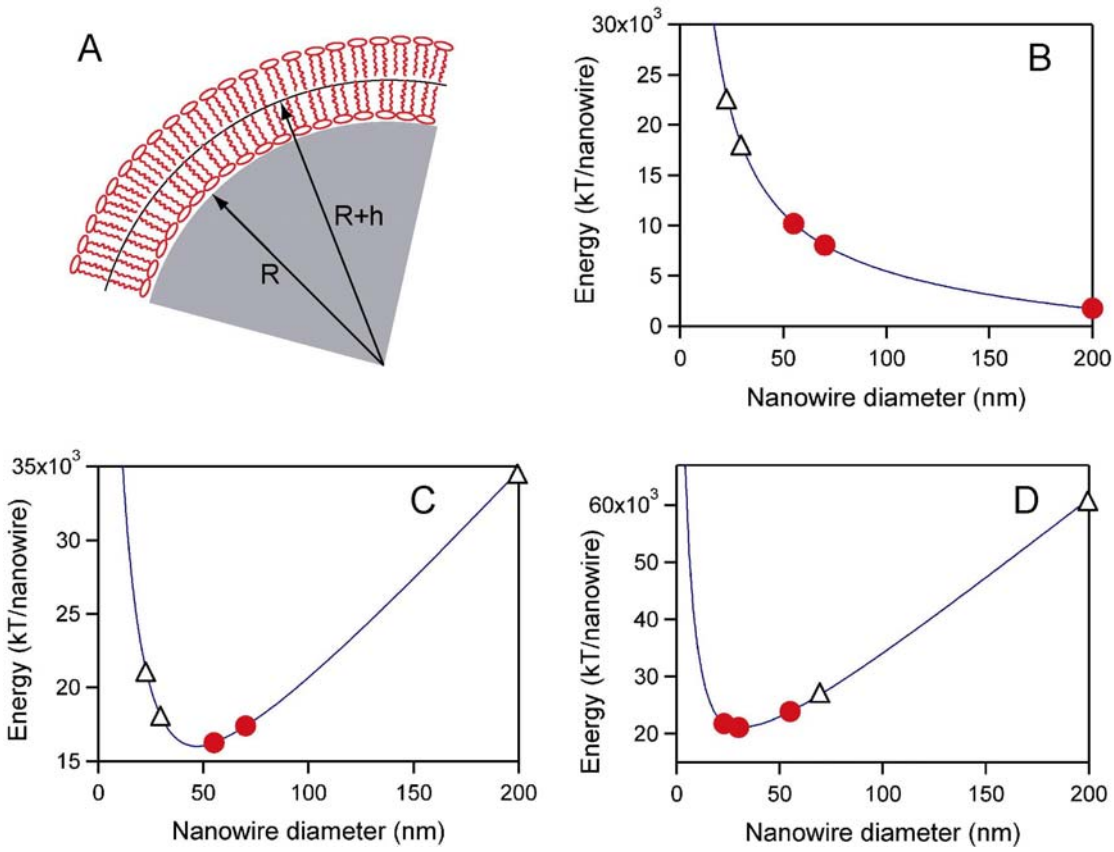

Figure 3. Thermodynamics of lipid bilayer formation on high curvature substrates. (**A**) Cross section of 1-D lipid bilayer on a nanowire substrate. (**B-D**) Change of the free energy of lipid bilayer formation on silicon nanowires (lines) for pure DOPC (**B**) and lipid mixtures with DOPC:DOPE ratio of 80:20 (**C**) and 70:30 (**D**). Open triangles correspond to the nanowire sizes where fusion does not occur while solid red circles correspond to the sizes where lipid bilayers form on the nanowires.

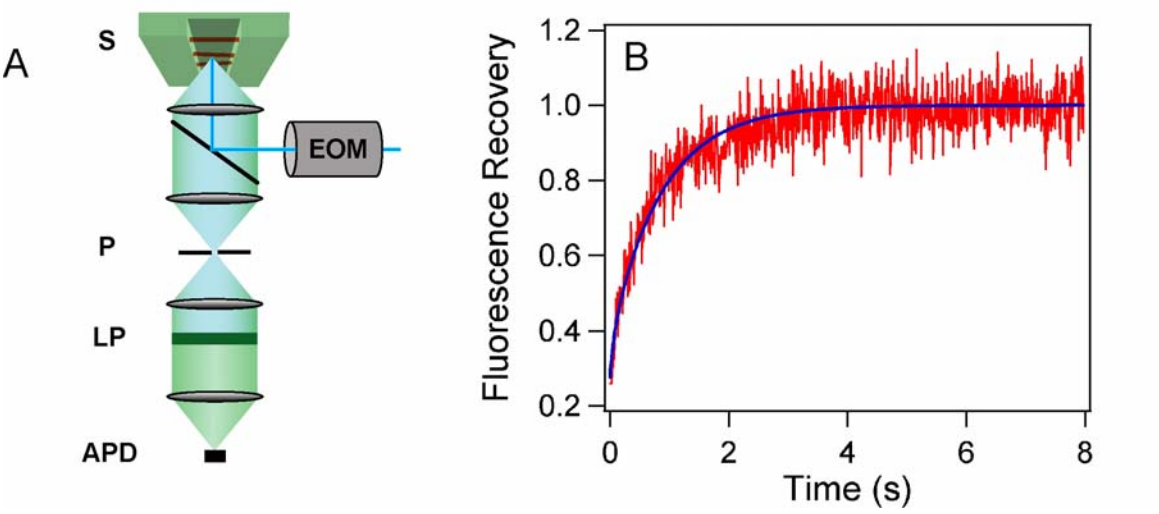

Figure 4. FRAP measurements of lipid mobility on nanowire supported lipid bilayers. (**A**) Schematic diagram of the experimental setup: S – sample, P – pinhole, LP – long pass filter, APD – avalanche photodiode detector, EOM – electro-optical modulator. (**B**) Representative fluorescence recovery curve (red) and the corresponding model fit (blue) for a nanowire supported DOPC bilayer. Nanowire diameter is 55 nm.